

Article

Multi-Phase Under Voltage Load Shedding Scheme for Preventing Delayed Voltage Recovery by Induction Motor Power Consumption Characteristics

Yunhwan Lee  and Hwachang Song * 

Department of Electrical and Information Engineering, Seoul National University of Science and Technology, Seoul 01811, Korea; yunan2@naver.com

* Correspondence: hcsong@seoultech.ac.kr; Tel.: +82-2-970-6403

Received: 22 June 2018; Accepted: 5 July 2018; Published: 10 July 2018



Abstract: This paper aims to develop a multi-phase under voltage load shedding (MUVLS) strategy that effectively sheds the load to mitigate delayed voltage recovery (DVR). The major cause of the DVR phenomenon is related to the dynamic characteristics of induction motor (IM) loads. The deaccelerating and stalling of the IM load during disturbances is the main driving force of short-term voltage instability, resulting in an amount of reactive power consumption and excessive current draw. With the economic efficiency of energy use, the proportion of IM loads is gradually increasing, and this trend might deteriorate system stability. This paper focuses on the impact of IM loads in the Korean power system and analyzes the parameter sensitivity of IM loads and the proportion of appropriate IM loads. The proposed procedure for under voltage load shedding (UVLS) applies voltage stability criteria to decide the most efficient load shedding scheme. The determined MUVLS scheme can offer new and more effective remedial actions to maintain voltage stability, considering the characteristics of IM loads. Case studies on the Korean power system have validated the performance of the proposed MUVLS scheme under severe contingency scenarios, showing that the proposed strategy effectively mitigates DVR.

Keywords: delayed voltage recovery; induction motor load; load configuration; inertia constant; voltage recovery criteria; under voltage load shedding; short term voltage stability

1. Introduction

The increased use of electronically controlled loads and the increasing induction motor (IM) loads make modern power systems more complex in terms of dynamic stability. The use of IM loads is continually evolving based on technological advances and economics, which changes the performance characteristics of the loads. The characteristics of IM-dominating loads have an important role in the dynamic behaviors of the systems. Recently, there has been an increasing concern on the load model of IMs, especially small single-phase IM loads for small appliances and some air conditioners (AC), and the portion of these is increasing. Systems with a large portion of inductive (IM) loads might face delayed voltage recovery (DVR) after the fault. The DVR phenomenon, observed and reported in various parts of the world, has been recognized as a voltage stability issue [1–4]. The phenomenon is basically caused by stalling of IM loads, and it could in turn potentially result in the cascading effect on other IMs in the same feeder or in their vicinity. As dynamic reactive power consumption by the IM loads stalling increases during disturbances, the imbalance between the reactive power supply and demand is aggravated. This might eventually cause voltage collapse in the power system. Thus, the growing penetration of IM loads in power systems is the leading driving force of short-term voltage instability [5–7].

The research on the DVR problems in the literature can be categorized into the following three aspects: (i) the development of a load model to represent DVR in time-domain simulation, (ii) the method to mitigate IM stalling in power systems, and (iii) the influence of the increasing distributed energy source (DER) penetration on the power system.

The literature related to the development of an IM load model can be reviewed as follows. The early studies on IM load modeling are summarized in [8,9]. In [10] and [11], the frame transformation and detailed flux modeling were proposed. They developed a set of differential equations for single-phase IM models that can be used in transient simulation [12]. A deterministic performance model based on experimental data was produced in [13]. IM stalling was studied probabilistically within the cascade model in [14,15]. The dynamic performance model for IM stalling and over-heat thermal tripping was developed in [16].

Generally, mitigation countermeasures against DVR events can be classified into supply side and demand side ones. As supply side countermeasures, utility applications include the implementation of flexible alternating current transmission system (FACTS) devices such as the static VAR compensator (SVC) and static synchronous compensator (STATCOM), for reactive power support [17–20]. As demand side countermeasures, under voltage load shedding (UVLS) has been widely used to mitigate voltage related problems [21]. In recent years, various UVLS schemes have been proposed. Regardless of a specific mechanism, the key parameters always are the time, the location, and the amount of load shedding for UVLS schemes [22–24]. However, the existing adaptive schemes do not consider the dynamics of motors [25,26].

The UVLS practices in the world [27] are as follows. In the North America, Puget Sound applies a distributed UVLS scheme using under-voltage relays as a safety net. New Mexico adopts the scheme preventing voltage collapse following loss of both 345 kV lines during peak loads. Entergy's scheme is against voltage collapse following critical double contingencies, and BC Hydro's scheme considers loss of major transmission or reactive power support facilities. Hydro Quebec applies a centralized scheme considering extreme disturbances. For Asia, TEPCO (Tokyo Electric Power Company) is applying prevent voltage collapse following extreme contingencies. The scheme of Taiwan Power Company is to estimate the load shedding amount based on the WECC's UVLS guidelines. For Europe, Spain implements a scheme of selectively shedding load based on a pre-determined criterion when imbalance of supply and demand is critical. Norway determines the load shedding amount based on offline analysis.

The installed capacity of DERs has increased significantly in industrialized countries in the last decade. High penetration of DERs could affect the power grid during system emergencies, potentially causing DVR events. One of the most important renewable power technologies is wind generation. A certain number of Type-1 induction generators are still operating in conventional wind farms. As a result, the dynamic behavior of induction machines has a significant impact on stability [28,29]. Wind generation facilities to DVR events are possibly exposed in the systems with a large amount of IM loads [30]. In [31], the effect of this problem was analyzed for the doubly fed induction generator (DFIG). The recent blackout event in South Australia clearly illustrated the catastrophic impact of DVR on a high-level wind energy penetrated power system [32]. A DVR problem was detected in [33] by a photovoltaic (PV) panel connecting to the power system, considering the impact of fault ride through (FRT) and dynamic reactive power support of large-scale PV systems on short-term voltage stability [34].

This paper analyzes the two aspects of modeling IM loads and countermeasures mitigating DVR, as well as the impact of IM loads on power systems. Since the proportion of IM loads is gradually increasing in today's power systems, transient voltage collapse due to short-term voltage instability might occur, and this can be a major threat to system security. The driving force of the problem is the tendency of aggregated IM loads to restore power consumption [23]. Thus, adequate IM modelling is very important to capture DVR phenomenon associated with short-term voltage stability (STVS). The DVR is directly related to the degree of IM-load penetration, especially that of residential air

conditioning (AC) in the power system. The U.S. Department of Energy (DOE) recognized the concerns of DVR events because of the increasing penetration of AC loads and started to deal with it as a national issue [35]. In the Republic of Korea, the demand for AC loads has grown significantly over the last few years, especially in summer seasons. The AC load in Korea occupies about 30% of the total load, and because of this the Korean power system might suffer from insufficient compensation of reactive power, possibly leading to an unacceptable voltage recovery after faults and critically to voltage collapse under summer peak load conditions.

The purpose of this study is to improve the understanding of IM load impacts and to identify the appropriate countermeasures to ensure stability of the power system. The widely used composite load model (ZIP + IM) is adopted in this paper for the system loads. This paper analyzes the sensitivity of the IM load parameters, and uses data from the statistical system to estimate the proportion of IM loads on the summer peak condition. In this paper, a multi-phase UVLS (MUVLS) scheme is proposed to improve the voltage stability. In the UVLS mitigation scheme, the dynamics of IM loads are considered, utilizing voltage stability determination conditions to determine the most efficient load shedding strategy. Employing MUVLS can mitigate the DVR caused by IM load power consumption characteristics, and it can improve system security in the most economical way.

2. Modeling and Problem Statement

For the stable operation of a power system, the balance between electrical inputs of the generator and electrical outputs of the system loads has to be kept all the time. Therefore, it is important to have an accurate knowledge about the characteristics of the load for stability analysis. For example, the load that consumes the power transmitted from the substations connected to the buses of the power system depends on the voltage and frequency. However, due to the complexity and diversity of the power system load, their modeling remains a challenging task. Therefore, such load modeling is needed that well represents the steady-state and transient behaviors of the physical loads of the systems. This paper adopts the composite load model, which is the combination of a static part with the constant impedance-current-power (ZIP) model and a dynamic part with the high-order IM model. The so-called ZIP plus IM model is widely employed because of the ability to express load dynamics accurately and its simple structure, and the model is especially used to analyze short-term voltage stability because dynamic response of loads is a key mechanism of it [23]. The detailed explanation of the composite load model can be found in [36–40], and it is explained in the following sections. The structure of the load model used in this paper is shown in Figure 1.

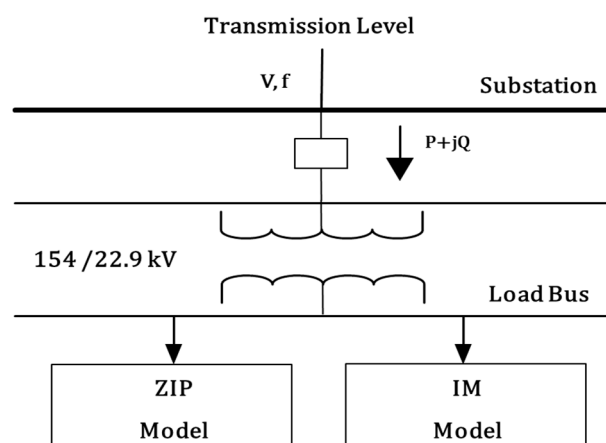


Figure 1. Composite load model (Constant impedance-current-power + Induction Motor).

2.1. Static Load Model

The static load model expresses the active and reactive powers at any instant of time as functions of the bus voltage magnitude and frequency at the same instant. The relationship between power and voltage magnitude of the model can be expressed as:

$$P = P_0 \left[a_P \left(\frac{V}{V_0} \right)^2 + b_P \left(\frac{V}{V_0} \right)^1 + c_P \right] \tag{1}$$

$$Q = Q_0 \left[a_Q \left(\frac{V}{V_0} \right)^2 + b_Q \left(\frac{V}{V_0} \right)^1 + c_Q \right] \tag{2}$$

where P_0 and Q_0 are respectively the active and reactive powers consumed at the reference voltage V_0 . In (1) and (2), the sum of coefficients for real power is 1, and that for reactive power is 1 as well.

2.2. Dynamic Load Model

The active and reactive powers in the dynamic load model are functions of the voltage magnitude and frequency at present and past time instants. For this purpose, several load models have been proposed in the literature, but the widely used one is the IM load model, because the physical system includes a large number of single-phase and three-phase IMs, and the IM model is included in stability simulation packages. In system studies, therefore, aggregated IM models are used. The IM loads are of the most significant aspects in terms of dynamical behaviors of the systems. As for the dynamic load behavior, the third-order IM model is employed. The equivalent circuit of the IM is shown in Figure 2.

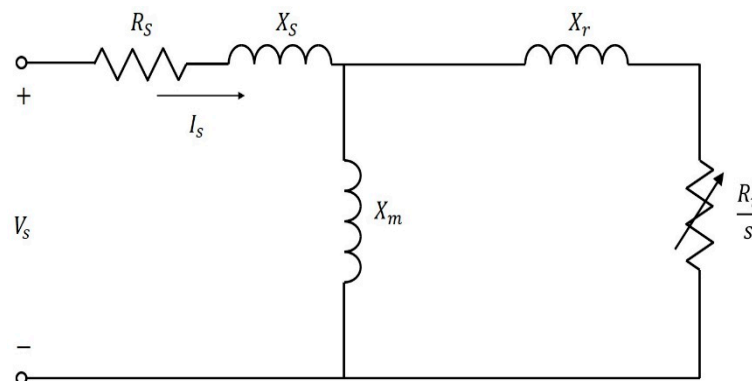


Figure 2. Induction motor equivalent circuit.

In Figure 2, V_s and I_s are the phasors for the IM terminal voltage and current, respectively; R_s , R_r , X_s and X_r are the resistances and reactances of the stator and rotor, respectively. X_m is the magnetizing reactance; s is the slip, which is $(\omega_0 - \omega) / \omega_0$, where ω_0 is the synchronous speed and ω is the rotor speed in electrical radians per second. The third-order model for the dynamic characteristics of an IM is represented by a differential equation representing the internal voltage (\overline{E}') in the d - q axis transformation, and a rotational equation representing the IM torque and the load torque.

$$\frac{dE'_d}{dt} = -\frac{1}{T'_0} [E'_d + (X - X')i_q] + \omega_0 s E'_q \tag{3}$$

$$\frac{dE'_q}{dt} = -\frac{1}{T'_0} [E'_q - (X - X')i_d] - \omega_0 s E'_d \tag{4}$$

$$\frac{ds}{dt} = \frac{1}{2H} (T_m - T_e) \tag{5}$$

$$i_d = \frac{1}{R_s^2 + X'^2} [R_s(v_d - E'_d) - X'(v_q - E'_q)] \tag{6}$$

$$i_q = \frac{1}{R_s^2 + X'^2} [R_s(v_q - E'_q) - X'(v_d - E'_d)] \tag{7}$$

where

$$T'_0 = (X_r + X_m) / \omega_0 R_r$$

$$T_e = E'_d i_d + E'_q i_q$$

$$X = X_s + X_m$$

$$T_m = T_{m0} [A(1 - s)^2 + B(1 - s) + C]$$

In the above equations, T'_0 is the transient time constant; X and X' are the synchronous reactance and transient reactance, respectively; E'_d and E'_q are d and q-axis transient voltages; I_d and I_q are d and q-axis stator currents; v_d and v_q are d and q-axis terminal voltages; H is the inertia constant of IM; T_m and T_e are mechanical and electromagnetic torque, respectively. The mechanical torque constants, A , B and C , are critical with respect to short-term voltage stability. T_{m0} is the torque when the motor is at synchronous speed.

2.3. Composite Load Model

The composite load model is used to accurately reflect the load characteristics of the practical system. The total real and reactive power are determined as:

$$P = P_s + P_m \tag{8}$$

$$Q = Q_s + Q_m \tag{9}$$

where P_s and Q_s are the active and reactive power of static load, and P_m and Q_m are the active and reactive power of dynamic load portion. The active and reactive power of the static load model part can be expressed as:

$$P_s = P_Z \left[a_p \left(\frac{V}{V_0} \right)^2 + b_p \left(\frac{V}{V_0} \right)^1 + c_p \right] \tag{10}$$

$$Q_s = Q_Z \left[a_q \left(\frac{V}{V_0} \right)^2 + b_q \left(\frac{V}{V_0} \right)^1 + c_q \right] \tag{11}$$

$$a_p + b_p + c_p = 1 - K_{pm} (K_{pm} = P_{motor} / P_{m0}) \tag{12}$$

$$a_q + b_q + c_q = 1 - K_{qm} (K_{qm} = Q_{motor} / Q_{m0}) \tag{13}$$

where P_Z and Q_Z are the real and reactive power of the load, respectively; P_{motor} and Q_{motor} are the initial real and reactive power of the IM; P_{m0} and Q_{m0} are the initial real and reactive power of the IM prior to the disturbance; K_{pm} and K_{qm} are the proportion of the IM in the total active and reactive load.

2.4. Development of Load Configuration for the Korean Power System

The analysis of the DVR phenomenon requires dynamic simulation based on appropriate representations of the loads, because the DVR phenomenon may occur due to the highly inductive characteristics of the small heating, ventilation, and air conditioning (AC) units, especially the AC loads. In summer peak conditions, AC loads can be a substantial dynamic factor of the DVR phenomenon, so the trend of gradual increase in the proportion of IM loads can critically impact on the system stability. Thus, determining accurate portion of IM loads of power systems is crucial. From the information on power consumption of system level, a valuable insight on the proportion of IM load can be obtained. In this paper, the IM proportion was decided based on the statistical information on

system load [41–43]. The proportion of IM loads in the system depends on a variety of factors, such as time and weather. As the reference, however, this paper uses the information on the load consumption for peak conditions, because this condition is the most severe in terms of voltage stability. Figure 3 shows the proportion of the IM loads in the total load at the summer peak each year.

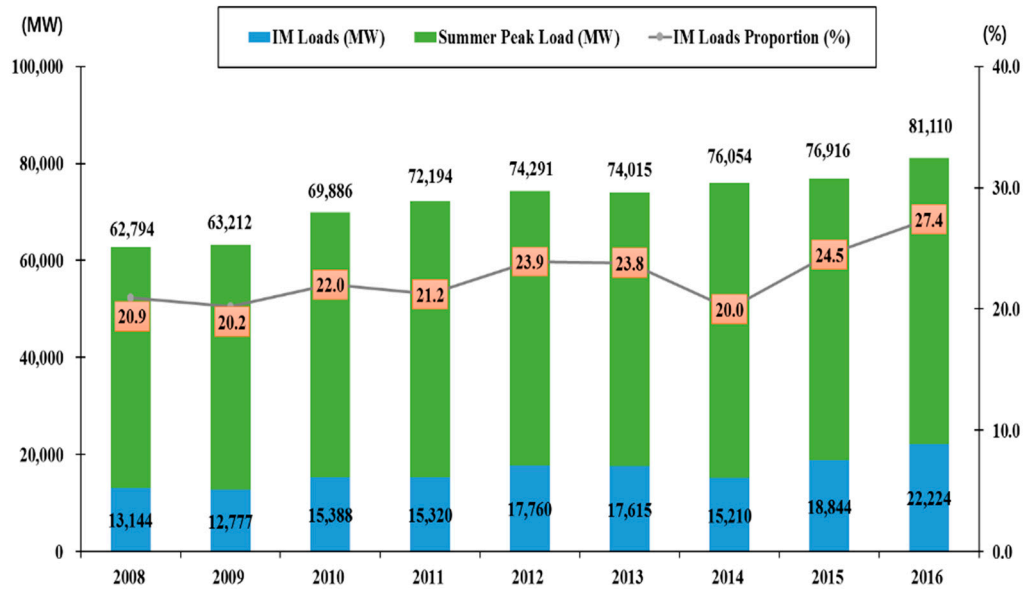


Figure 3. IM load proportion at summer peak condition.

From Figure 3, one can notice that the proportion of IM loads in the system load shows a steady increase over the years. The consumption of IM loads becomes 27.4% in 2016. The increasing tendency of supply and use of IM loads directly affects the maximum demand. Also, an increase in the IM loads might cause an imbalance between the supply and demand, resulting in degrading the energy utilization efficiency and deteriorating the stable supply of electric power.

The factors for the increase in the IM loads are as follows. One factor contributing to this consumption is the climate conditions. The reliability and load capability of the power systems can be affected by climate change. Another factor exacerbating the problem is the increasing peak electricity demand. The demand on Korean power systems has increased in recent years. Thus, one of the major causes of this problem is AC loads. The third factor is the changes in household type, such as the increase in single-person households, which is the main cause of the increase in electricity power demand. Because AC is regarded as an essential appliance for a basic life in the hot and humid Korean summer, the use of cooling equipment is expected to rise. These factors are expected to further increase in the proportion of future AC loads. Based on the above-mentioned data, it can be seen that the IM load in the Korean Power System could reach more than 30% of the total load. Load modeling considering IM loads in summer peak conditions is reasonable for simulation for DVR problems.

This paper performs dynamic simulations using the composite load model. Based on the actual load configuration, a recalculated data of the proportion of the ZIP and IM loads was created and applied to the dynamic simulation. The concepts of reflecting the ZIP and IM loads proportion in practical system data can be expressed as shown in Figure 4.

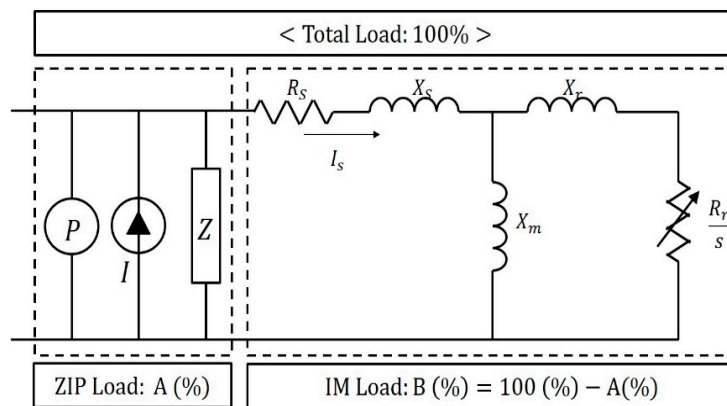


Figure 4. Proportion of the ZIP and IM load.

2.5. Problem Statement

Recently, the DVR phenomenon has been a critical issue in terms of voltage stability because IM load penetration is growing significantly. When an AC load stalls, it behaves as a constant shunt conductance and reactance consuming active and reactive power, and motor stalling might also cause the tripping of transmission lines and transformers because of an increase in system impedance. In such conditions, sufficient reactive power cannot be transmitted to the load. Also, this problem would be aggravated by the growing use of low inertia IM loads in the transmission grid network. After the fault, for a system with a high proportion of IM loads, the problem can be spread throughout the system, resulting in wide-area blackouts [7].

For the Korean power system, there is little literature on the DVR phenomenon and the impact assessment considering the characteristics of the IM load. That is, the current UVLS scheme does not reflect the DVR and the behaviors of IM loads. IM load models are not incorporated in dynamic simulations, and this makes it difficult to capture the DVR phenomenon, even though the proportion of IM load in the actual load configuration is increasing. For detailed simulations, representing large and small IM loads in various combinations is needed, because the IM load is sensitive to dynamic variation in voltage and frequency. When designing the UVLS scheme, the time, the location and the amount of load shedding needs to be determined. For the current UVLS scheme of the Korean system, the total amount of load shedding is decided only based on the results of steady-state analysis, and it is applied at once when the pick-up under voltage condition is satisfied. The control amount of load shedding is sometimes excessive when the post-disturbance condition is not much severe, and then in this case over voltage problem can happen. Also, the UVLS scheme is tested with transient stability simulation packages without considering IM load portion, so it could not capture the DVR problem when the amount of load shedding is not enough, because of a slightly large time delay. Thus, this paper proposes an approach to decide the multi-phase UVLS (MUVLS) scheme, considering an adequate portion of IM load, as well as the DVR problem. The MUVLS scheme can provide proper remedial actions in a reliable and economic way for various post-disturbance conditions.

3. Analysis of IM Loads Characteristics in Power System

3.1. IM Load Parameter Sensitivity Analysis

This paper performs sensitivity analysis of the IM load parameters and their effect on the system voltage. Mentioned above in Section 2, the IM load model comprises six parameters; R_s , R_r , X_s , X_r , and X_m are all in [p.u.] but H is in [second]. Figure 5 shows the time trajectories of bus voltages as the result of time-domain analysis considering the voltage recovery characteristics with regard to the changes in IM load parameters.

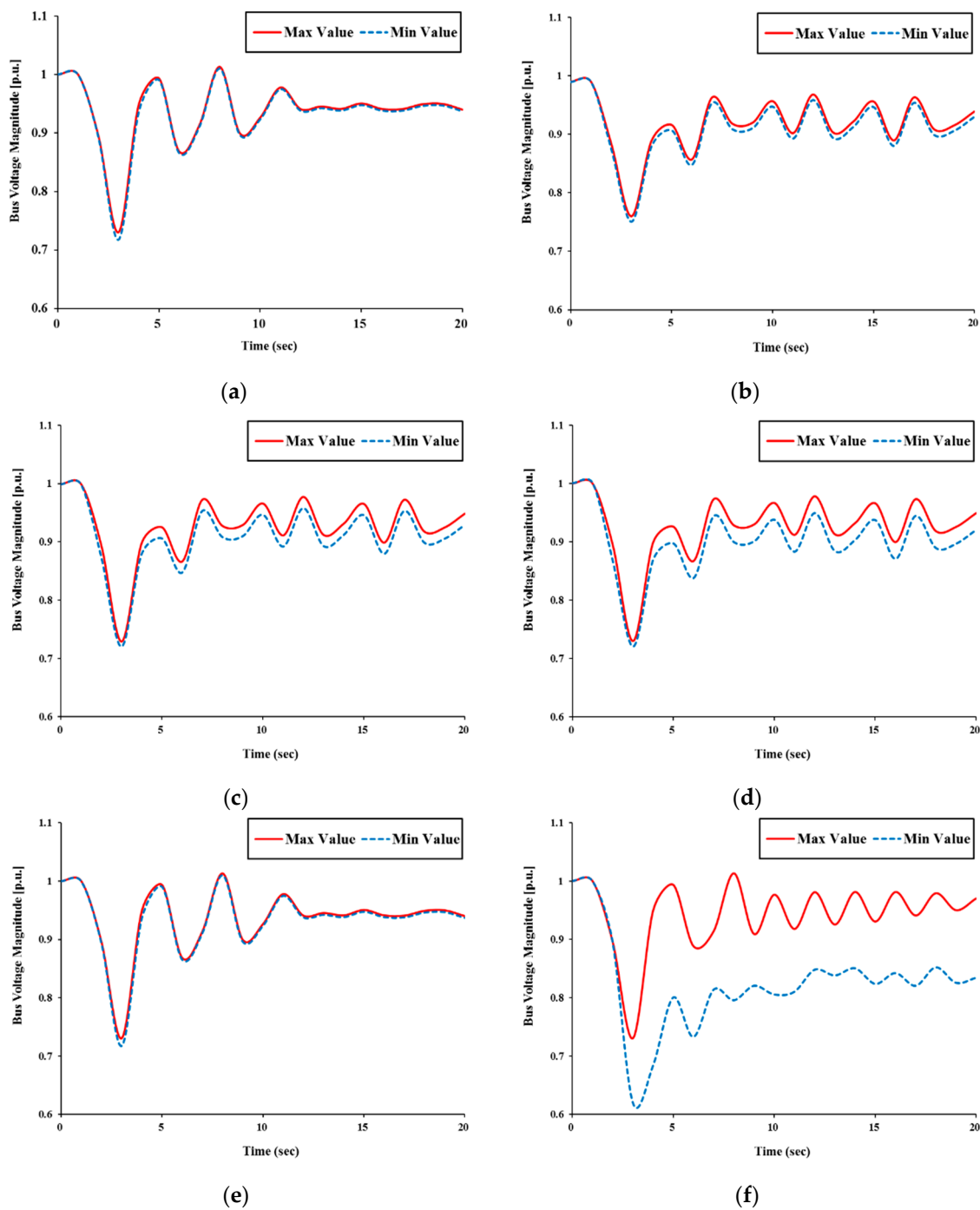


Figure 5. Bus voltage sensitivity analysis results of IM parameters. (a) R_s ; (b) X_s ; (c) R_r ; (d) X_r ; (e) X_m ; (f) H .

From Figure 5, one can notice that the bus voltage profiles are not very sensitive with regard to the changes in R_s , R_r , X_s , X_r , and X_m . On the other hand, the inertia constant H had an influence on the system voltage. When the H value is high, the fluctuation of the bus voltage becomes large; this means that the power system’s voltage recovery ability is closely affected by H . The inertia constant H can be expressed as:

$$H = \frac{\text{Kinetic energy at synchronous speed}}{\text{MVA power base}} = \frac{\frac{1}{2}I\omega_0^2}{S_{base}} \tag{14}$$

where I is the moment of inertia; and S_{base} is the MVA power base. Although the inertia constant varies depending on the machine’s capacity and type, the values range from 1 to 10 [second]. For a rotating load, the motor can be either directly connected or through a gear or belt drive [30]. The swing equations can be expressed as follows:

$$\frac{2H}{\omega_0} \dot{\omega} = T_m - T_e \tag{15}$$

From the swing equations, Equation (5) of the IM model can be derived. It is noted that increasing load results in an increase of slip [23]. In the form of kinetic energy, the power system has its own energy level because several machines in the power system rotate with speeds close to ω_0 . From the definition of the inertia constants with rated powers of individual generators, the kinetic energy level can be obtained as follows:

$$KE_{sys} = \sum_{i=1}^N S_{ni} H_{si} \tag{16}$$

where S_{ni} is the rated power of the generator; and H_{si} is the inertia constant of the synchronous generator i . Not only synchronous generators, but also induction machines in service contribute to the kinetic energy. Then, the system kinetic energy KE_{sys} can be calculated as follows:

$$KE_{sys} = \sum_{i=1}^N S_{ni} H_{si} + \sum_{i=1}^N IM_{ni} H_{mi} \tag{17}$$

where IM_{ni} is the proportion of IM; and H_{mi} is the inertia constant of induction machines. When the system has a high IM proportion, the kinetic energy of the power system might be decreased, compared to cases only with synchronous generators. In high IM load concentrated regions, consumption of reactive power is high. As a result, the equivalent inertia of the system decreases, and this has a significant impact on the system’s dynamical responses. In this paper, dynamic characteristic analysis is performed by the mean of changing H values as well as the proportion of IM loads.

3.2. Voltage Recovery Characteristics of IM Loads

Typically, the IM loads can be categorized based on their capacity (large and small) and load type. It might be desirable to model IM loads with both small and large motors, with significantly different parameters depending on their sizes [9,44]. When only considering the parameters for large IM loads, the corresponding load portion can be regarded as being too large, so the system’s margin seems to be high. When only taking into account those for small IM loads, the industrial IM load might be too small, so the simulation results seem to be more critical than the real system’s behavior. For this reason, dynamic characteristic analysis is needed, considering the intermediate values for the parameters, and the values used in this paper are as shown in Table 1.

Table 1. Parameters of induction motor loads.

R_s	X_s	R_r	X_r	X_m	H
0.043	0.074	0.025	0.051	3.14	0.4~1.6

The IM loads are about 60% to 70% of the total load for a typical power system, but applying this IM portion can provide critical simulation results. In simulation, the most widely used portions are 40% or 50%. In this paper, based on the above-mentioned data, it is recommended that the range of the IM portion is from 30% to 50% to get reliable simulation results. This paper also reflects the characteristics of H regarding power system stability. Table 2 shows the results of the analysis on the voltage recovery characteristics depending on the proportion of the IM loads and the H parameter changes.

Table 2. Result of induction motor loads proportion and *H* parameter changes.

IM Loads Proportion (%)	<i>H</i> Parameter						
	0.4	0.6	0.8	1.0	1.2	1.4	1.6
30	●	●	○	○	○	○	○
40	●	●	●	○	○	○	○
50	●	●	●	●	●	●	●

Voltage Recovery: ○/Voltage Instability: ●.

When the applied proportion of IM loads was 30% or 40%, it can be seen that the voltage recovery characteristics were similar, regardless of the change of *H*. When the proportion of IM loads was 50% and the *H* value was increased, voltage instability occurred. The power system voltage did not recover due to the generator angle stability problem. A low value of *H* becomes a severe situation, but a high value of *H* makes the situation of the systems less severe. When the IM loads suffer a sustained low voltage, they consume excessive reactive power. According to the results, the equilibrium point of the system did not exist. In addition, if fault clearing was not quickly applied, the kinetic energy of the IM load was increased and the voltage could not be recovered. This short-term voltage instability problem is greatly affected by the proportion of IM loads. If the proportion is low, the voltage recovery is fast, but if the proportion is high, the voltage recovery might be slow, or the system might experience voltage collapse [30]. Figure 6 shows the results of the effect of IM load proportion on the system behaviors, assuming that the proportion of IM loads is about 30–50%.

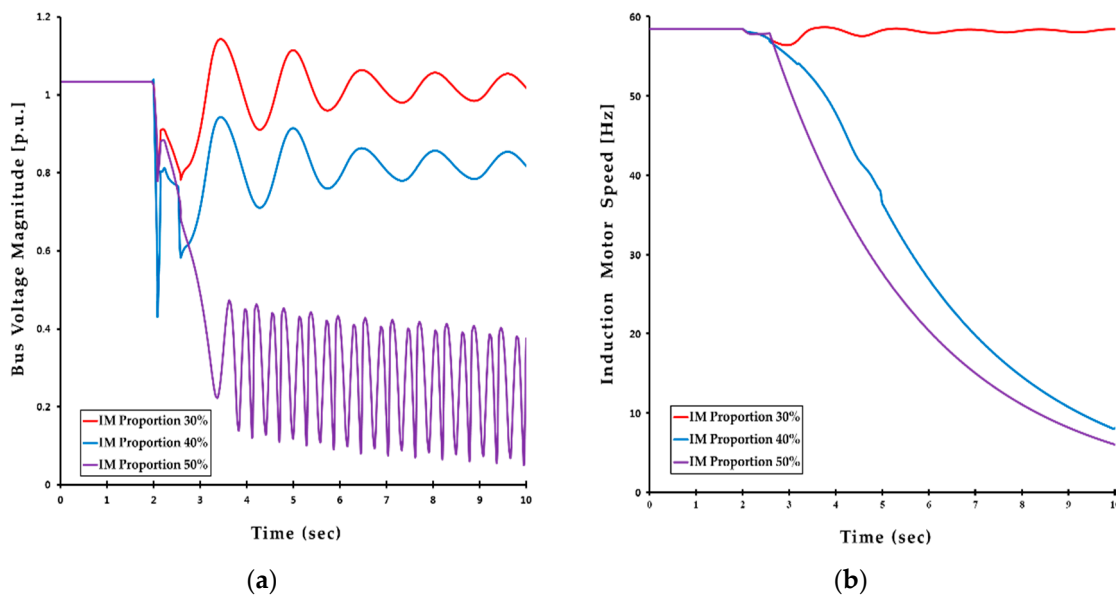


Figure 6. Effect of IM loads proportion on power systems. (a) Bus voltage magnitude. (b) IM speed.

From Figure 6, in the case of an IM proportion of 30%, the bus voltage was stabilized after the fault was cleared. The IM load speed successfully has been recovered to a normal speed, and the IM loads are reaccelerated. In the case of an IM proportion of 40%, the stalling of IM loads occurred after the fault. For the high IM load condition, motors could not reaccelerate. The IM load speed did not recover to the normal speed due to the fact that the IM mechanical and electrical torque curves did not intersect, and the IM slip exceeded the unstable equilibrium point. In the case of an IM proportion of 50%, the voltage instability happened by the stalling of the IM loads after the fault. IM load speed dropped due to the increase in the total transmission impedance. As a result, IM stalling caused voltage collapse because of the post-fault equilibrium point not existing.

3.3. Voltage Recovery Criteria

When a power system is prone to short-term voltage instability, fast reactive support near the load center is essential. The reactive support should be able to restore a stable equilibrium point under severe contingency, and it should be fast, before the IM load decelerates beyond the post-control unstable equilibrium point. IM loads will usually stall when subjected to low voltages due to a fault, even for a very fast clearing time. However, IM loads away from the fault location can ride through faults without stalling if the fault is cleared fast enough.

UVLS is the ultimate countermeasure for short-term voltage instability. This scheme is used to prevent the stalling of IM loads [23]. To evaluate the voltage recovery of the power system, a transient voltage recovery criterion (TVRC) is required. The objectives of a voltage recovery criterion are to ensure fault ride through by the majority of the loads and to minimize the risk of motor stalling. The authors of [3,45] proposed a TVRC for the transmission system; however, they did not consider the delayed voltage recovery problem (e.g., IM stalling) in the transmission system. Based on the TVRC transmission system developed by PJM [46], modified criteria were established in this paper and the criteria were applied to the transient voltage recovery characteristics of the Korean power system. In the modified criteria, the time of voltage-recovering up to 95% of the nominal values after the clearing of a fault is added. Table 3 shows the determination of the established voltage stability conditions.

Table 3. Determination of voltage stability conditions.

Condition	Description	Criteria
1	Following the clearing of a fault, time to recover voltage to up to 95% of their nominal values.	Recovery Time within 2 s
2	Following the successful clearing of a fault, the voltage magnitudes should be no less than 70% of their nominal values.	Satisfaction (○)/Dissatisfaction (●)
3	Within 20 cycles following the clearing of a fault, the voltage magnitudes should be no less than 80% of their nominal values.	
4	Within 0.5 s following the clearing of a fault, the voltage magnitudes should be no less than 90% of their nominal values	
5	Within 1.5 s following the clearing of a fault, the voltage magnitudes should be no less than the steady-state voltage minimum, typically 92–95% of nominal.	

If the voltage recovered slower than the criteria given in the above conditions, load shedding should be performed. Based on the conditions, this paper establishes a load shedding scheme to prevent short-term voltage instability.

4. Results and Discussion

4.1. Multi-Phase Under Voltage Load Shedding Scheme Strategy

The Korean power system has a structure in which most of the electric power is generated from non-metropolitan areas and load consumption is concentrated in the Seoul metropolitan area. For this reason, high-voltage interface lines are required to supply power to the metropolitan area from non-metropolitan areas. The interface lines are composed of four routes of 345 kV lines and two routes of 765 kV lines. However, the increase in active power flow via the interface lines due to the economical purpose inevitably leads to voltage instability in cases where reactive power is not adequately supported in the metropolitan area. Also, the Korean power system has a critical constraint with the interface flow, which is mainly determined by voltage stability. Thus, when the most severe 765 kV transmission line faults occur, to prevent voltage instability, the UVLS system might be needed. The UVLS system monitors the voltage of the main substations in the metropolitan area and the tripping of the 765 kV transmission line after faults. It is designed to shed a predetermined 1500 MW

load in the metropolitan area when voltage falls below a predefined level. However, the UVLS system does not consider the voltage recovery characteristics of the load. Because the load shedding amount is determined under the maximum load conditions, unnecessary load amounts might be shed.

This paper proposes a MUVLS scheme to prevent excessive load shedding based on CLM (ZIP plus IM model), and the scheme will improve the short-term voltage stability issue in the Korean power system. The CLM is used to simulate the phenomenon of DVR. The dynamics of IM loads are fully considered, so the voltage stability condition is identified. Considering the IM loads in the power system, the voltage recovery and slip characteristics are influenced by the fault clearing time. The difference in the voltage recovery characteristics can be caused by the different fault clearing time. Even with a short time difference, the load shedding time after the fault has a significant influence on the voltage instability. In order to establish the MUVLS strategy, a review was made on the load shedding amount (LSA) and the load shedding time (LST) for each of the phases 1, 2, and 3. Table 4 shows the case study for the selection of LSA and LST.

Table 4. Case study for selection of LSA and LST.

Case	Phase-1 LSA (%)	Phase-1 LST (second)	Phase-2 LSA (%)	Phase-2 LST (second)	Phase-3 LSA (%)	Phase-3 LST (second)
A ¹	40	0.5	30	1.0	30	1.5
B ¹	50	0.5	30	1.0	20	1.5
C ¹	60	0.5	40	1.0		
D ²	40	0.4	30	0.8	30	1.2
E ²	50	0.4	30	0.8	20	1.2
F ²	60	0.4	40	0.8		
G ⁴	40	0.3	30	1.0	30	1.5
H ⁴	50	0.3	30	1.0	20	1.5
I ⁴	60	0.3	40	1.0		
J ⁵	40	0.3	30	0.8	30	1.2
K ⁵	50	0.3	30	0.8	20	1.2
L ⁵	60	0.3	40	0.8		
M ¹	40	0.3	30	0.8	30	1.3
N ¹	50	0.3	30	0.8	20	1.3
O ¹	60	0.3	40	0.8		
P ²	40	0.3	30	0.7	30	1.1
Q ²	50	0.3	30	0.7	20	1.1
R ²	60	0.3	40	0.7		
S ³	40	0.3	30	0.6	30	0.9
T ³	50	0.3	30	0.6	20	0.9
U ³	60	0.3	40	0.6		

¹ Time step: 0.5 s/² Time step: 0.4 s/³ Time step: 0.3 s/⁴ Phase 2, 3 time step: 0.5 s/⁵ Phase 2, 3 time step: 0.4 s.

As it checks whether the voltage has been stably recovered or not, the LSA and LST are changed. To ensure short-term voltage stability, load shedding should be completed within 1.5 s after the fault. For this purpose, to select the LST, the maximum time is set to 1.5 s and the minimum time to 0.9 s. Phase-1 LSA and LST are selected, as LST is increased from 0.3 s, pursuing the lowest LSA and shortest LST. Figure 7 shows that the bus voltage recovery depends on LSA and LST.

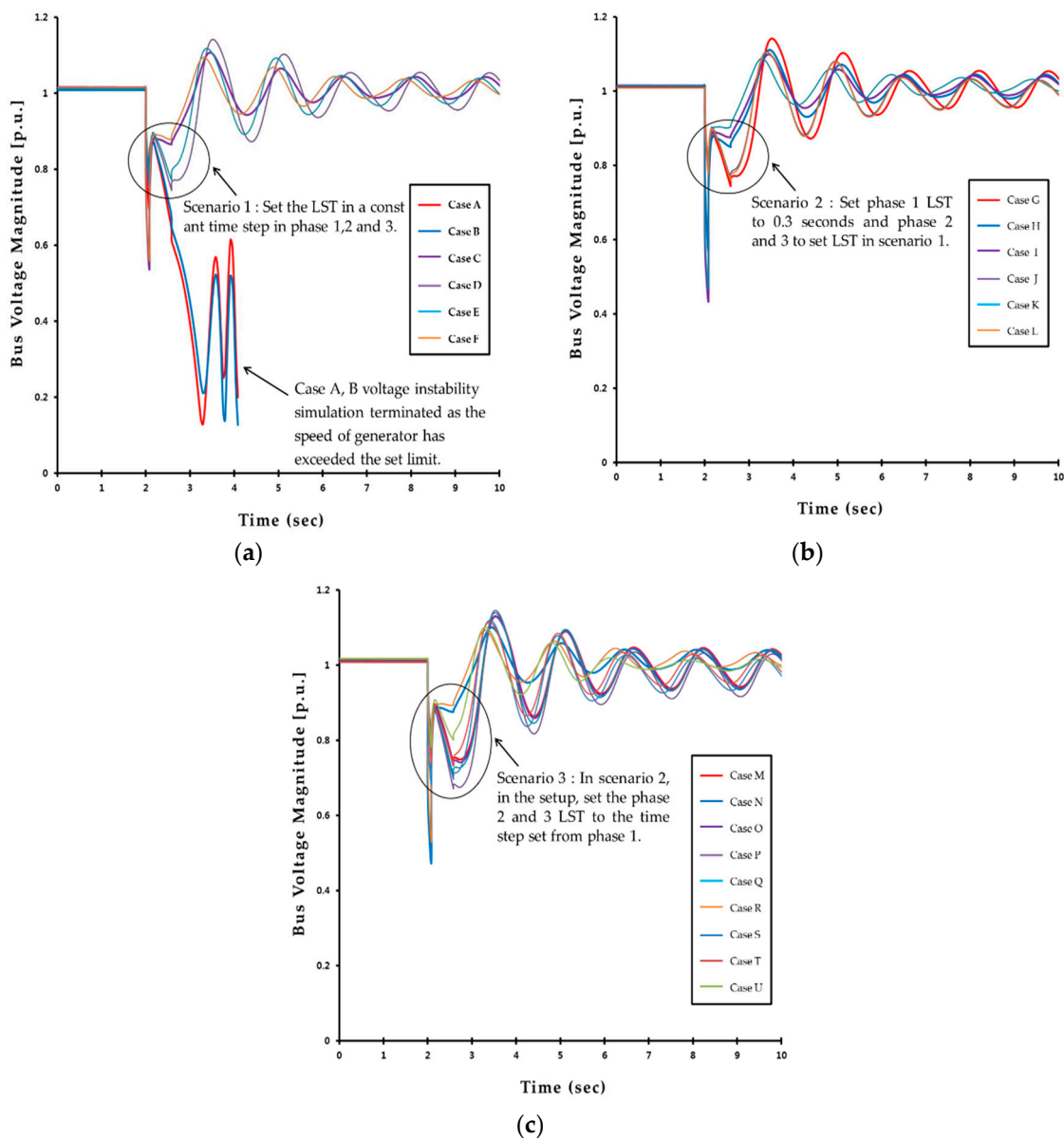


Figure 7. Results of bus voltage recovery depends on load shedding amount (LSA) and load shedding time (LST). (a) Scenario 1: Set the LST in a constant time step in phase 1, 2 and 3; (b) Scenario 2: Set phase 1 LST to 0.3 s and phase 2 and 3 to set LST in scenario 1; (c) Scenario 3: In scenario 2, in the setup, set the phase 2 and 3 LST to the time step set from phase 1.

From Figure 7, one can notice that when applying case A and B for the MUVLS scheme, voltage instability occurs. For these cases, the full deployment time is 1.5 s. Although load shedding is applied in phase 1, the LST is long, so that the kinetic energy of the IM load is significantly increased, resulting in voltage instability. Case C increased the LSA in phase 1 despite the longer LST, and the final LST was applied within 1 s after the fault, resulting in stable voltage recovery. It can be seen that as the initial LSA decreased, the importance of fast load shedding increased. Cases D–U show the result of voltage recovery, but it can be seen that the phase-2 and phase-3 LSA and LST do not affect the voltage recovery. As a result, it can be seen that phase-1 LSA and LST significantly impact the voltage recovery. The selected LSA and LST of the MUVLS control strategy based on Case S, which has the lowest LSA and the fastest LST per phase in the above results.

The decision for load shedding is usually made by system operators, based on pre-established practical criteria. However, the existing UVLS scheme does not consider the dynamics of IM loads. When severe faults are applied to the systems, motor stalling might happen due to the reduced rotation speed of IMs. Because the existing UVLS scheme only considers the ZIP model in dynamic analysis, the effect of motor stalling on voltage recovery cannot be reflected by the scheme. For systems with a high portion of IM load, voltage reduction below a certain level after disturbances might cause voltage instability or DVR. To reduce load interruption, in this situation, adequate countermeasures should be taken, such that the controlled load shedding schemes and countermeasures should be carefully determined, considering the dynamical behaviors of IM loads. Comparison results of bus voltage recovery for existing schemes and the proposed scheme are shown in Figure 8.

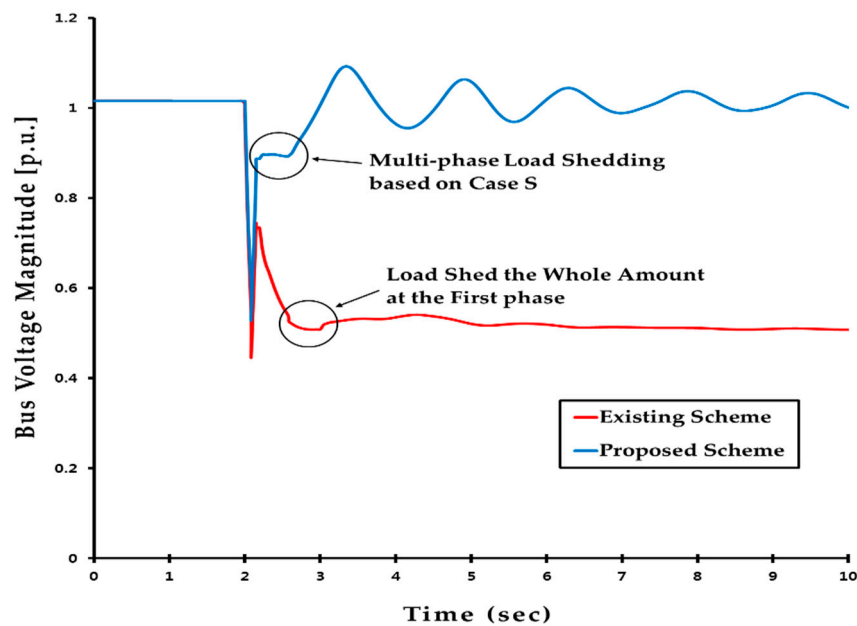


Figure 8. Comparison results of bus voltage recovery for existing scheme and proposed scheme.

When designing UVLS schemes, proper determination of LSA and LST is essential. Practically, LSA is selected by steady-state analysis, and LST by dynamic analysis. The existing UVLS scheme for the Korean power system is based on the chosen LSA, and it sheds the whole control amount at the first phase. However, this might be excessive. In addition, the approach is based on the premise that there is no transient instability or transient behavior in system voltage. To ensure short-term voltage stability, therefore, LSA and LST need to be determined by both steady-state and dynamic analysis. As the situation of the power system changes in real time, if the MUVLS is applied, the LSA can be reduced compared to the existing scheme. The LSA and LST can be properly determined using the MUVLS strategy, lowering shedding amount for a better performance of voltage recovered.

4.2. Case Studies

In this study, the objectives of the simulation are to determine the adequate IM load proportion in the Korean power system. In addition, the MUVLS control strategy was applied to a practical system in order to verify the DVR mitigation effectiveness. Case studies on the Korean power system have validated the performance of the proposed MUVLS scheme under severe contingency scenarios. As mentioned earlier, the proportion of IM loads occupied about 30% under summer peak conditions. Therefore, since the proportion of IM loads is expected to increase continuously due to abnormal weather conditions, to perform dynamic analysis simulations of the appropriate proportion at which the power system could stabilize, the IM load proportion was increased by 1% from 30%.

When applying the proposed MUVLS strategy, the process monitors whether to satisfy the voltage stability condition. If this condition is satisfied, it is possible to discuss the adequate proportion at which the dynamic characteristics of the IM loads can restore the voltage of the power system to ensure short-term voltage stability. Figure 9 shows the flowchart of the algorithm for the method proposed in this paper.

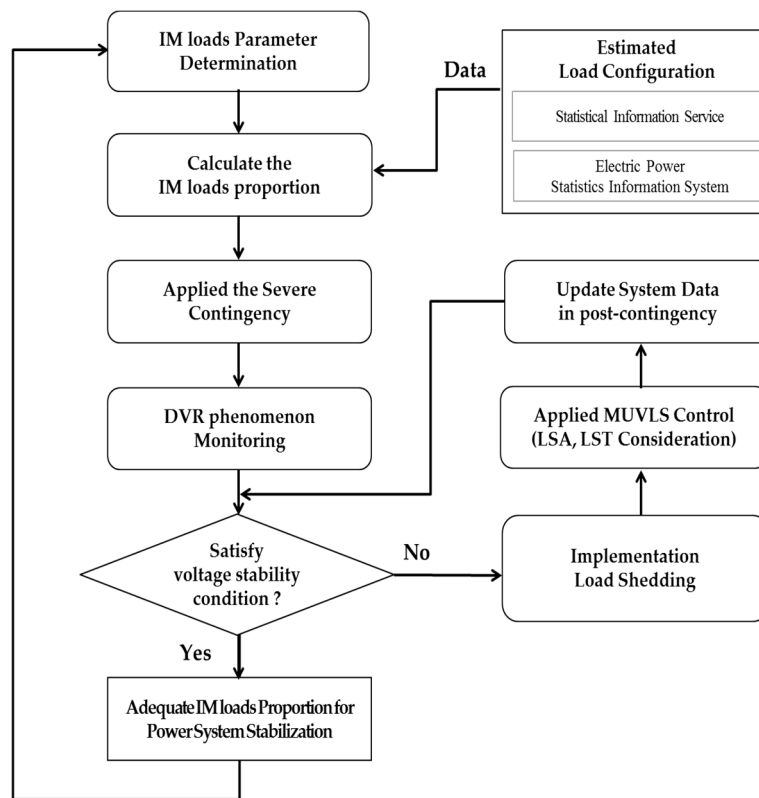


Figure 9. Flowchart of the proposed multi-phase under voltage load shedding (MUVLS) strategy.

IM load proportion 30–34% cases did not satisfy voltage stability conditions without performing load shedding. In order to satisfy the criteria shown in Table 3, MUVLS was performed for each case. Table 5 shows the voltage stability condition satisfaction status at post-contingency after the load shedding.

Table 5. Voltage stability condition satisfaction status after the load shedding.

Condition	IM Loads Proportion (%)				
	30	31	32	33	34
1	○	○	○	○	○
2	○	○	○	○	○
3	○	○	○	○	○
4	○	○	○	●	●
5	○	○	○	●	●
Status	Satisfaction (stability)			Dissatisfaction (instability)	

Figure 10 shows the stability condition satisfaction status after the load shedding and voltage recovery with MUVLS at severe contingency.

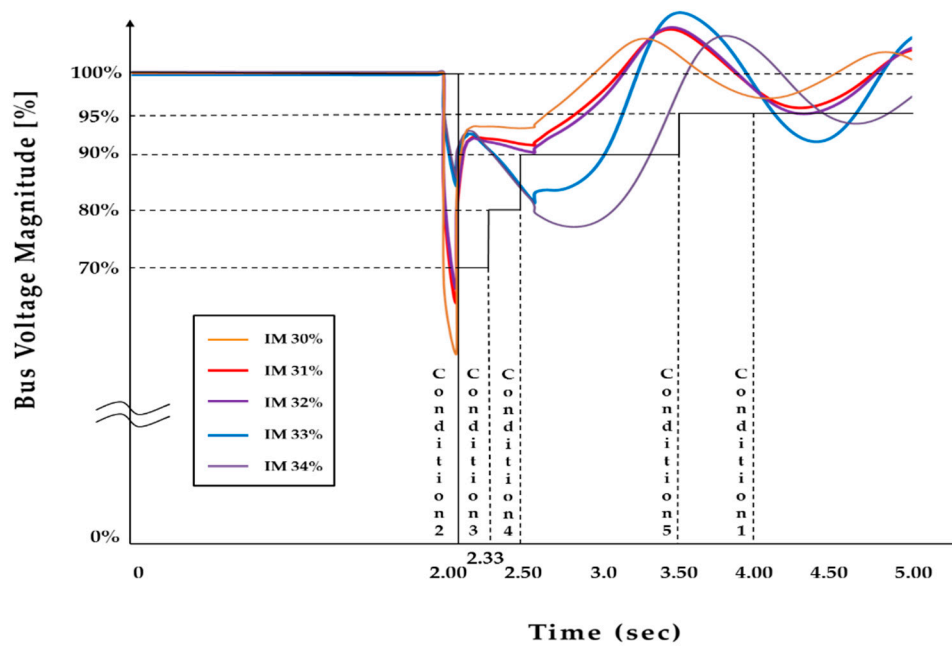


Figure 10. Voltage recovery with MUVLS at severe contingency.

From Figure 10, the cases satisfying all of the voltage stability conditions are those in which the IM load proportions were below 32%. When the proportion of IM loads is greater than 33% of the power system load, voltage instability due to the DVR phenomenon occurs. It can be seen that the power system voltage recovers with proportions less than 33%. As the proportion of the IM loads decreases, the number of buses satisfying the voltage stability condition increases. This dynamic analysis clearly shows that setting the adequate proportion in Korea to about 32% improves the short-term voltage stability. The result can be used as a basic reference for AC load management in Korean power systems. However, it is necessary to consider the diverse situations of Korean power systems.

Due to the improved standards of living, the AC, with its convenience of use, is becoming so popular in Korea that the AC loads are continuously increasing. The impact of relatively cheap electric home appliance pricing on the convenience of electrical energy is leading to inefficiency in energy use. The supply and use patterns of AC loads will have a significant impact on power demand in the summer season. As a result, the increased use of AC loads directly affects the increase in maximum power, and this tends to have an important impact on future power systems. In addition, the concentration of the power use of AC loads is coincident with the maximum power demand, in most cases. Because a reasonable management of power use for the HVAC system (especially AC loads) is essential for stable power supply, it is necessary to use objective data that are actually being gathered through surveys. Considering this situation, the existing load management system should also be strengthened by introducing a peak pricing policy that temporarily raises price rates significantly during peak hours (3 to 4 h per day, 4 weeks per year) in summer to ensure a stable power supply. It is necessary to strengthen load management by conducting surveys on AC loads, and as an alternative to electric cooling, it is desirable to develop a technology to actively distribute gas cooling and adjust the electricity pricing. Additionally, a management and control system for DER and controllable loads is required, and for this purpose, control methods should be developed to achieve adequate voltage regulation as in [47,48].

5. Conclusions

In this paper, we proposed a MUVLS strategy to improve the short-term voltage stability issue through improvement in power system operation technology in a scenario where the AC load supply

is expected to increase rapidly. When the stalled motors were tripped from the grid, the voltage entered the delayed recovery condition. The voltage recovery response is a very important dynamic characteristic of load behaviors. A method to improve the system reliability in terms of voltage and reactive power was proposed for increasing AC load penetration. The main contribution of this paper is that the applied scheme controls load shedding to mitigate the DVR caused by the power-consumption characteristics of IM loads. From the simulation results, it was possible to confirm that the power system stability is directly related to the inertial constant H . In addition, a dynamic analysis of IM loads with a voltage recovery characteristic was secured to determine and verify the adequate proportion of such loads in the power system. The dynamic simulation results showed that the proposed scheme was effective under severe fault conditions, and the extensive results fully demonstrated the effectiveness of MUVLS in voltage instability conditions and that it improved short-term voltage stability. The MUVLS strategy to contribute to improving the short-term voltage stability while effectively controlling the IM loads and securing the power systems.

Future research work will focus on development of a real-time UVLS scheme using the PMU (Phasor Measurement Unit) due to detailed monitoring of DVR events. It is necessary to study real-time measurement equipment that can accurately perform decision-making and reflect the state of severity of the power system. If applying the UVLS method based on PMU, it is possible to take adequate countermeasures in case of serious or unexpected fault within the system. PMU is used for operational preparations and DVR mitigation. In addition, electrical end-use characteristics are changing rapidly, as more loads become electronically connected. Many power electronic loads (DER, EV) have constant power characteristics with respect to voltage magnitudes, which could degrade the power system voltage stability. Therefore, it is also necessary to study their impacts on power system short-term voltage stability.

Author Contributions: Y.L. conceived and designed the research, performed the system simulations, and wrote the paper; H.S. supervised the research and improved the system simulations and made suggestions for this research.

Funding: This research received no external funding.

Acknowledgments: This research was supported by Human Resources Development of the Korea Institute of Energy Technology Evaluation and Planning (KETEP) grant funded by the Korea government Ministry of Trade, Industry & Energy (20174030201840).

Conflicts of Interest: The authors declare no conflicts of interest.

References

1. Dong, Y.; Xie, X.; Wang, K.; Zhou, B.; Jiang, Q. An emergency-demand-response based under speed load shedding scheme to improve short-term voltage stability. *IEEE Trans. Power Syst.* **2017**, *32*, 3726–3735. [[CrossRef](#)]
2. Paramasivam, M.; Salloum, A.; Ajarapu, V.; Vittal, V.; Bhatt, N.B.; Liu, S. Dynamic optimization based reactive power planning to mitigate slow voltage recovery and short term voltage instability. *IEEE Trans. Power Syst.* **2013**, *28*, 3865–3873. [[CrossRef](#)]
3. Bai, H.; Ajarapu, V. A novel online load shedding strategy for mitigating fault-induced delayed voltage recovery. *IEEE Trans. Power Syst.* **2011**, *26*, 294–304. [[CrossRef](#)]
4. Glavic, M.; Novosel, D.; Heredia, E.; Kosterev, D.; Salazar, A.; Habibi-Ashrafi, F.; Donnelly, M. See it fast to keep calm: Real-time voltage control under stressed conditions. *IEEE Power Energy Mag.* **2012**, *10*, 43–55. [[CrossRef](#)]
5. De Leon, J.D.; Taylor, C.W. Understanding and solving short-term voltage stability problems. In Proceedings of the Power Engineering Society Summer Meeting, Chicago, IL, USA, 21–25 July 2002; Volume 2, pp. 745–752.
6. Al-Mubarak, A.H.; Bamsak, S.M.; Thorvaldsson, B.; Halonen, M.; Grunbaum, R. Preventing voltage collapse by large SVCs at power system faults. In Proceedings of the 2009 IEEE/PES Power Systems Conference and Exposition, Seattle, WA, USA, 15–18 March 2009; pp. 1–9.

7. Alaqeel, T.A.; Almohaimeed, S.A.; Suryanarayanan, S. A review of air conditioning motor loads stalling on voltage recovery in the Saudi electric grid. In Proceedings of the Power Symposium (NAPS), Morgantown, WV, USA, 17–19 September 2017; pp. 1–6.
8. Price, W.W.; Casper, S.G.; Nwankpa, C.O.; Bradish, R.W.; Chiang, H.D.; Concordia, C.; Wu, G. Bibliography on load models for power flow and dynamic performance simulation. *IEEE Power Eng. Rev.* **1995**, *15*, 70.
9. Price, W.W.; Taylor, C.W.; Rogers, G.J. Standard load models for power flow and dynamic performance simulation. *IEEE Trans. Power Syst.* **1995**, *10*, 1302–1313.
10. Stankovic, A.M.; Lesieutre, B.C.; Aydin, T. Modeling and analysis of single-phase induction machines with dynamic phasors. *IEEE Trans. Power Syst.* **1999**, *14*, 9–14. [[CrossRef](#)]
11. Bravo, R.; Yinger, R.; Chassin, D.; Huang, H.; Lu, N.; Hiskens, I.; Venkataramanan, G. *Final Project Report Load Modeling Transmission Research*; Lawrence Berkeley National Laboratory (LBNL): Berkeley, CA, USA, 2010.
12. Liu, Y.; Vittal, V.; Undrill, J.; Eto, J.H. Transient model of air-conditioner compressor single phase induction motor. *IEEE Trans. Power Syst.* **2013**, *28*, 4528–4536. [[CrossRef](#)]
13. Tomiyama, K.; Daniel, J.P.; Ihara, S. Modeling air conditioner load for power system studies. *IEEE Trans. Power Syst.* **1998**, *13*, 414–421. [[CrossRef](#)]
14. Wu, H.; Dobson, I. Cascading stall of many induction motors in a simple system. *IEEE Trans. Power Syst.* **2012**, *27*, 2116–2126. [[CrossRef](#)]
15. Wu, H.; Dobson, I. Analysis of induction motor cascading stall in a simple system based on the CASCADE model. *IEEE Trans. Power Syst.* **2013**, *28*, 3184–3193. [[CrossRef](#)]
16. Zheng, H.; DeMarco, C.L. A New Dynamic Performance Model of Motor Stalling and FIDVR for Smart Grid Monitoring/Planning. *IEEE Trans. Smart Grid* **2016**, *7*, 1989–1996. [[CrossRef](#)]
17. Sullivan, D.; Pape, R.; Birsa, J.; Riggle, M.; Takeda, M.; Teramoto, H.; Kono, Y.; Temma, K.; Yasuda, S.; Wofford, K.; et al. Managing fault-induced delayed voltage recovery in Metro Atlanta with the Barrow County SVC. In Proceedings of the Power Systems Conference and Exposition, Seattle, WA, USA, 15–18 March 2009; pp. 1–6.
18. Meliopoulos, A.S.; Cokkinides, G.; Stefopoulos, G. Voltage stability and voltage recovery: Load dynamics and dynamic VAR sources. In Proceedings of the Power Systems Conference and Exposition, Atlanta, GA, USA, 29 October–1 November 2006; pp. 124–131.
19. Hsu, S.M. Design and application of a static VAR compensator for voltage support in the Dublin, Georgia area. In Proceedings of the 2005/2006 IEEE/PES Transmission and Distribution Conference and Exhibition, Dallas, TX, USA, 21–24 May 2006; pp. 1399–1406.
20. Du, M.; Han, M.; Cao, Z.; Chu, F.; Ei-Kady, M. Utilizing STATCON to resolve delayed voltage recovery problem in SEC-WR. In Proceedings of the Asia-Pacific Power and Energy Engineering Conference, Wuhan, China, 28–31 March 2009; pp. 1–4.
21. Taylor, C.W. Concepts of undervoltage load shedding for voltage stability. *IEEE Trans. Power Deliv.* **1992**, *7*, 480–488. [[CrossRef](#)]
22. Mollah, K.; Bahadornejad, M.; Nair, N.K.; Ancell, G. Automatic under-voltage load shedding: A systematic review. In Proceedings of the 2012 IEEE Power and Energy Society General Meeting, San Diego, CA, USA, 22–26 July 2012; pp. 1–7.
23. Van Cutsem, T.; Vournas, C. *Voltage Stability of Electric Power Systems*; Springer Science & Business Media: New York, NY, USA, 1998; Volume 441.
24. Ladhani, S.S.; Rosehart, W. Under voltage load shedding for voltage stability overview of concepts and principles. In Proceedings of the Power Engineering Society General Meeting, Denver, CO, USA, 6–10 June 2004; pp. 1597–1602.
25. Saffarian, A.; Sanaye-Pasand, M. Enhancement of power system stability using adaptive combinational load shedding methods. *IEEE Trans. Power Syst.* **2011**, *26*, 1010–1020. [[CrossRef](#)]
26. Tang, J.; Liu, J.; Ponci, F.; Monti, A. Adaptive load shedding based on combined frequency and voltage stability assessment using synchrophasor measurements. *IEEE Trans. Power Syst.* **2013**, *28*, 2035–2047. [[CrossRef](#)]
27. IEEE PES Power System Relaying Committee. *Working Group C-13, System Protection Subcommittee-Undervoltage Load Shedding Protection*; IEEE PES Power System Relaying Committee: Minneapolis, MN, USA, 28 June 2010.

28. Zamani, M.H.; Fathi, S.H.; Riahy, G.H.; Abedi, M.; Abdolghani, N. Improving transient stability of grid-connected squirrel-cage induction generators by plugging mode operation. *IEEE Trans. Energy Convers.* **2012**, *27*, 707–714. [CrossRef]
29. Wang, D.; Yuan, X.; Zhang, M. Power-Balancing Based Induction Machine Model for Power System Dynamic Analysis in Electromechanical Timescale. *Energies* **2018**, *11*, 438. [CrossRef]
30. North American Electric Reliability Corporation. *Technical Reference Paper Fault-Induced Delayed Voltage Recovery*; 2009.
31. Borges, R.C.; Ramos, R.A. Analysis of the influence of the FIDVR problem in the operation of a DFIG under unbalanced conditions. In Proceedings of the 2016 IEEE PES Transmission & Distribution Conference and Exposition-Latin America (PES T&D-LA), Morelia, Mexico, 20–24 September 2016; pp. 1–6.
32. Operator, A.E.M. *Black System, South Australia, 28 September 2016. Power System Operating Incident Reports*; Australian Energy Market Operator: Melbourne, Australia, 2017.
33. Miller, N.W.; Shao, M. Active control of distribution connected photovoltaic systems for reduction of fault-induced delayed voltage recovery. In Proceedings of the CIRED Workshop, Rome, Italy, 11–12 June 2014; pp. 1–4.
34. Lammert, G.; Boemer, J.C.; Premm, D.; Glitza, O.; Ospina, L.D.P.; Fetzer, D.; Braun, M. Impact of fault ride-through and dynamic reactive power support of photovoltaic systems on short-term voltage stability. In Proceedings of the 2017 IEEE PowerTech, Manchester, UK, 18–22 June 2017; pp. 1–6.
35. On the Role of Residential AC Units in Contributing to Fault-Induced Delayed Voltage Recovery. In Proceedings of the U.S. Department of Energy Workshop, Irving, TX, USA, 22 April 2008.
36. Arif, A.; Wang, Z.; Wang, J.; Mather, B.; Bashualdo, H.; Zhao, D. Load Modeling—A Review. *IEEE Trans. Smart Grid* **2017**. [CrossRef]
37. Kim, J.K.; An, K.; Ma, J.; Shin, J.; Song, K.B.; Park, J.D.; Park, J.W.; Hur, K. Fast and reliable estimation of composite load model parameters using analytical similarity of parameter sensitivity. *IEEE Trans. Power Syst.* **2016**, *31*, 663–671. [CrossRef]
38. Boemer, J.C.; Rawn, B.G.; Gibescu, M.; van der Meijden, M.A.; Kling, W.L. Response of wind power park modules in distribution systems to transmission network faults during reverse power flows. *IET Renew. Power Gener.* **2015**, *9*, 1033–1042. [CrossRef]
39. Son, S.; Lee, S.H.; Choi, D.H.; Song, K.B.; Park, J.D.; Kwon, Y.H.; Hur, K.; Park, J.W. Improvement of composite load modeling based on parameter sensitivity and dependency analyses. *IEEE Trans. Power Syst.* **2014**, *29*, 242–250. [CrossRef]
40. Price, W.W.; Chiang, H.D.; Clark, H.K.; Concordia, C.; Lee, D.C.; Hsu, J.C.; Srinivasan, K. Load representation for dynamic performance analysis. *IEEE Trans. Power Syst.* **1993**, *8*, 472–482.
41. Widjaja, I.; Latulipe, D.; D’Aquila, D.; Ng, G.; Swe, K. *SS-38 Load Modeling Working Group Progress Report*; North American Electric Reliability Corp: Atlanta, GA, USA, 2016.
42. Korean Statistical Information Service. Available online: <http://kosis.kr/index/index.do> (accessed on 8 May 2018).
43. Electric Power Statistics Information System. Available online: <http://epsis.kpx.or.kr/epsisnew/> (accessed on 10 May 2018).
44. Kundur, P.; Balu, N.J.; Lauby, M.G. *Power System Stability and Control*; McGraw-hill: New York, NY, USA, 1994; Volume 7.
45. Halpin, S.M.; Harley, K.A.; Jones, R.A.; Taylor, L.Y. Slope-permissive under-voltage load shed relay for delayed voltage recovery mitigation. *IEEE Trans. Power Syst.* **2008**, *23*, 1211–1216. [CrossRef]
46. PJM Transmission Planning Department. *EXELON Transmission Planning Criteria*; PJM Transmission Planning Department: Philadelphia, PA, USA, 2009.
47. Zheng, W.X.; Han, Q.L. Distributed Energy Management for Smart Grids with an Event-Triggered Communication Scheme. *IEEE Trans. Control Syst. Technol.* **2018**, *PP*, 1–12.
48. Ding, L.; Han, Q.L.; Wang, L.Y.; Sindi, E. Distributed cooperative optimal control of DC microgrids with communication delays. *IEEE Trans. Ind. Inform.* **2018**. [CrossRef]

